Creating bound states in excitable media by means of nonlocal coupling

Grigory Bordyugov* and Harald Engel
Institut für Theoretische Physik, Technische Universität Berlin, Hardenbergerstrasse 36, 10623 Berlin, Germany
(Received 4 April 2006; revised manuscript received 11 May 2006; published 17 July 2006)

We consider pulses of excitation in reaction-diffusion systems subjected to nonlocal coupling. This coupling represents long-range connections between the elements of the medium; the connection strength decays exponentially with the distance. Without coupling, pulses interact only repulsively and bound states with two or more pulses propagating at the same velocity are impossible. Upon switching on nonlocal coupling, pulses begin to interact attractively and form bound states. First we present numerical results on the emergence of bound states in the excitable Oregonator model for the photosensitive Belousov-Zhabotinsky reaction with nonlocal coupling. Then we show that the appearance of bound states is provided solely by the exponential decay of nonlocal coupling and thus can be found in a wide class of excitable systems, regardless of the particular kinetics. The theoretical explanation of the emergence of bound states is based on the bifurcation analysis of the profile equations that describe the spatial shape of pulses. The central object is a codimension-4 homoclinic orbit which exists for zero coupling strength. The emergence of bound states is described by the bifurcation to 2-homoclinic solutions from the codimension-4 homoclinic orbit upon switching on nonlocal coupling. We stress that the high codimension of the bifurcation to bound states is generic, provided that the coupling range is sufficiently large.

DOI: 10.1103/PhysRevE.74.016205 PACS number(s): 05.45.−a, 82.40.Ck, 47.54.−r

I. INTRODUCTION

Propagation of pulses in excitable media is an important phenomenon in physical, chemical, and biological systems, including chemical reactions, signal propagation in neuronal tissue, brain activity, and calcium waves in living cells [1]. Typically such pulses can propagate due to local diffusive coupling between the excitable elements of the medium. The interaction between two pulses that propagate in the same direction is usually repulsive, which means that the second pulse in a pulse pair runs more slowly than the first one [2].

However, pulses in reaction-diffusion systems do not always interact only repulsively, but can form so-called bound states with two or more pulses that propagate at the same velocity. Such bound states were found in chemical reaction-diffusion systems experimentally [3–6]. A kinematic approach was introduced in Refs. [7,8], where the existence of bound states was closely related to the anomalous dispersion of periodic pulse trains.

The main motivation for the consideration of nonlocal coupling comes from neuroscience—it was shown that neurons communicate by means of long-range interactions [9,10]. Nonlocal coupling plays an important role in certain electrochemical reactions [11,12] as well. Recent theoretical findings include the improvement of synchronization of coupled oscillators [13], emergence of completely new dynamical regimes (the so-called chimera states) [14], spiral waves with randomized core [15], chemical turbulence induced by nonlocal coupling [16], and many others. Nicola *et al.* reported a codimension-2 Turing-wave bifurcation and a region of bistability between Turing and wave patterns resulting from inhibitory nonlocal coupling [17,18]. Spiral patterns on a stationary background have been observed recently in experiments with the Belousov-Zhabotinsky reaction under influence of nonlocal coupling with short-rage activation and long-range inhibition [19]. For the Oregonator model of the Belousov-Zhabotinsky reaction it has been shown that nonlocal coupling can induce Turing and wave instabilities of the homogeneous steady state. While a long-range activation was found to induce travelling waves, long-range inhibition leads to stationary Turing patterns [20]. While most of the results on the impact of nonlocal coupling obtained so far are related to the instabilities of the homogeneously steady state, in this paper we focus on the effect of nonlocal coupling on the interaction of propagating excitation pulses.

The main result of the present paper is the following. Suppose that we have a reaction-diffusion system that supports propagation of solitary pulses of excitation, which interact repulsively through their monotonic refractory tails. Introducing nonlocal coupling in the form of a convolution of the pulse profile with an exponentially decaying kernel results in the attractive interaction of pulses and the emergence of bound states. Regardless of the particular excitable kinetics, bound states bifurcate from the primary solitary pulse at nonlocal coupling strength $\mu=0$. More specifically, we show that the solitary pulse for $\mu=0$ is represented by a homoclinic orbit of codimension-4, which is unfolded upon setting $\mu\neq 0$. In this description, bound states are represented by 2-homoclinic orbits which bifurcate at $\mu=0$ from the primary one, corresponding to the solitary pulse. We illustrate our analysis by numerical calculations with a model for the light-sensitive Belousov-Zhabotinsky reaction [21].

From the mathematical viewpoint, the stability theory of multibump pulses (bound states of pulses) and weak interaction of pulses are developed in Ref. [22] and thoroughly reviewed in a more general context in Ref. [23]. The mathematical background for the bifurcation and the existence of bound states is provided by the theory of codimension-2 bifurcations of homoclinic orbits in $\mathbb{R}^N$, $N\geq 3$, see Ref. [24].

*Electronic address: greg@physik.tu-berlin.de

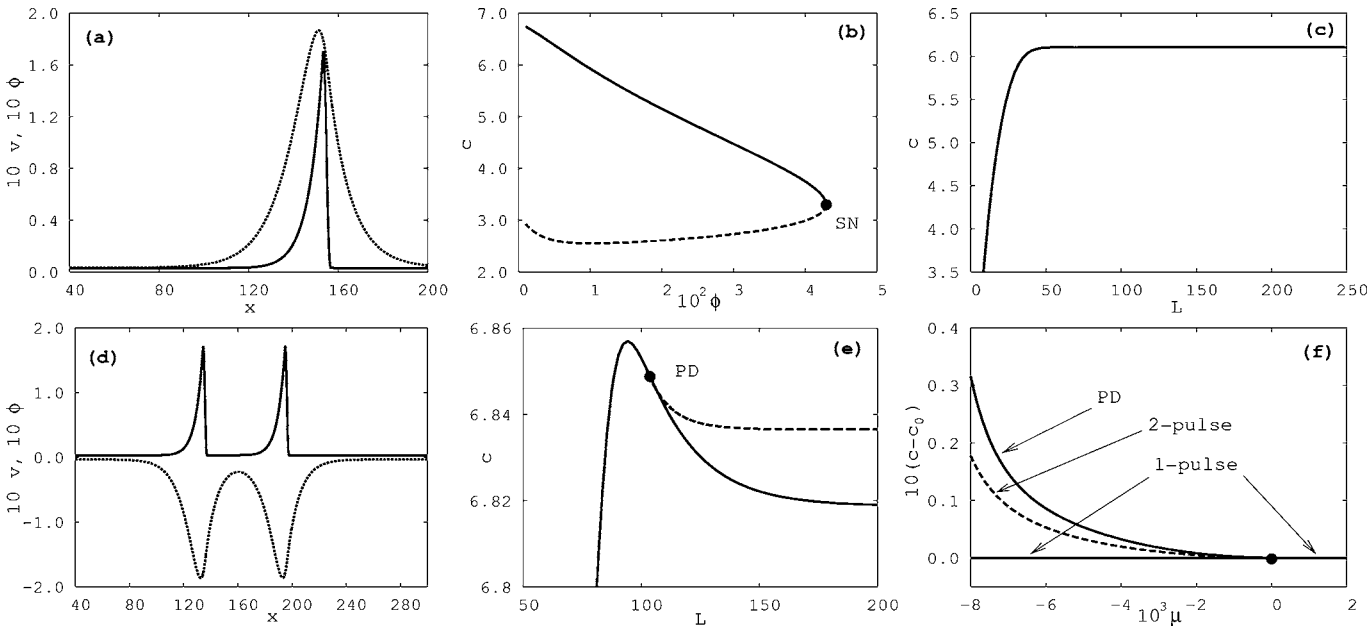

FIG. 1. (a) Profile of a solitary pulse in Eq. (1) for $\mu=0$, where rescaled variable $v(x)$ is shown by the solid line and the rescaled value of the integral in Eq. (2) is shown by the dashed line. (b) Dependence of the velocity of a solitary pulse c on the parameter ϕ_0. Solid (dashed) line represents stable (unstable) solitary pulses, respectively. (c) Dispersion curve of spatially periodic pulse trains for $\mu=0$ showing the velocity of pulse train c versus the interpulse distance L. (d) Profile of a bound state for $\mu=-8.0\times10^{-3}$, solid and dashed line show rescaled $v(x)$ and rescaled $\phi(x)$, respectively. (e) Dispersion curve for $\mu=-8.0\times10^{-3}$. Point *PD* indicates period doubling, see text. Dashed line displays the dispersion curve for pulse trains with doubled interpulse distance. (f) Relative velocity of two-pulse solutions (dashed line) and that of the pulse trains that undergo the period-doubling bifurcations *PD* (solid line) in comparison with the velocity of solitary pulse c_0 versus the nonlocal coupling strength μ.

For a review and analytical description of codimension-2 homoclinic orbits in a simple toy model see Ref. [25] and references therein. We refer also to Refs. [26,27] for codimension-3 resonant flip bifurcations.

This paper is organized as follows. First, we present our numerical observations on bound states in the Oregonator model with nonlocal coupling and give a simple model-specific explanation how these bound states come into play due to nonlocal coupling. Then we consider an abstract reaction-diffusion equation with nonlocal coupling and show that the emergence of bound states occurs independently on the specific kinetics of the model. In our considerations we will need some essential results on the codimension-2 bifurcations of homoclinic orbits, which will be discussed briefly in Sec. III B.

II. RESULTS WITH OREGONATOR MODEL

A. Emergence of bound states

We consider first solitary pulses in the Oregonator model for the excitable light-sensitive Belousov-Zhabotinsky reaction [28]

$$\partial_t u = \epsilon^{-1}\left[u - u^2 - (fv + \phi)\frac{u-q}{u+q}\right] + \partial_{xx}u,$$

$$\partial_t v = u - v, \tag{1}$$

subjected to a nonlocal coupling through the field $\phi(x)$ of characteristic coupling range $\sigma^{-1} \gg 1$ and strength μ

$$\phi(x) = \phi_0 + \mu\int_{-\infty}^{\infty} e^{-\sigma|y|}[v(x+y) - v(x)]dy. \tag{2}$$

The activator variable u is proportional to the concentration of bromous acid and the inhibitor v represents the oxidized form of the catalyst. In this section, we fix the parameters values as follows: $\epsilon^{-1}=20$, $f=2.1$, $q=0.002$, $\phi_0=0.008$, $\sigma=0.1$. This choice of the parameters corresponds to excitable local dynamics of Eq. (1).

With the above set of parameters and $\mu=0$, Eq. (1) supports propagation of stable solitary pulses of excitation, see Fig. 1(a). The parameter ϕ_0 describes an additional light-induced inhibitor production and setting it to larger values makes the pulses of excitation propagate slower [Fig. 1(b)], which will be an important fact for our considerations later on. From this viewpoint, $\mu>0$ corresponds to an inhibitory nonlocal coupling, while choosing $\mu<0$ makes nonlocal coupling (2) be of an activatory type.

Without nonlocal coupling (i.e., for $\mu=0$), pulses in Eq. (1) interact only repulsively, which can be seen from the positive slope of the dispersion curve for pulse trains with large interpulse distances [Fig. 1(c)]. Upon switching on the coupling strength to the value $\mu=-8.0\times10^{-3}$, we observe that pulses do not interact repulsively anymore, but can in contrast form bound states with two pulses propagating at the same velocity [Fig. 1(d)]. Our numerical computations show that the emerged bound state is linearly stable, see next section. The dispersion curve for spatially periodic pulse trains for $\mu=-8.0\times10^{-3}$ displays an overshoot followed by a do-

main with a negative slope [Fig. 1(e)]. Near the maximum of the dispersion curve we find a period-doubling bifurcation that corresponds to the emergence of nonequidistant pulse trains.

Plotting the relative velocity of the double-pulse solution (i.e., compared to the velocity of the solitary pulse c_0 for the same value of μ) and that of the period-doubling bifurcation versus the coupling strength μ, we see that the two-pulse solutions and the period-doubling bifurcation stem exactly from the point $\mu=0$ [Fig. 1(f)]. The interpulse distance of the pulse trains that undergo the period-doubling bifurcation *PD* approaches infinity for $\mu\to 0$ (not shown in figures).

Using the fact that the field $\phi(x)$ acts as a second inhibitor in Eq. (1), we can give a heuristic explanation for the emergence of bound states. For $\sigma^{-1}\gg 1$, the profile of $\phi(x)$ is much broader in comparison with $u(x)$ and $v(x)$, and the interaction of pulses within a bound state is dominated by the interaction of the second pulse with the ϕ wake of the first pulse. If $\mu>0$, the values of $\phi(x)$ are larger than ϕ_0, and the ϕ wake of the first pulse slows down the second one, making bound states impossible. In the case of $\mu<0$, the profile of $\phi(x)$ behind the first pulse approaches ϕ_0 from below, which effectively makes the second pulse propagate faster until it abuts against the stronger inhibitory tail of the variable $v(x)$. We stress that for every negative $\mu\to 0$ there exist a bound state, since for large interpulse distance the attracting interaction with longer tail of ϕ always dominates the repulsive interaction with the faster decaying inhibitory v tail.

Summarizing the results with the Oregonator model, we conclude that bound states emerge due to the interplay between long-range attraction through the nonlocal coupling and short-range repulsion, provided by the inhibitory wake of the variable v behind the pulse.

B. Stability of bound states

We computed the linear stability of bound states, in which we linearized the reaction-diffusion system Eq. (1) with the nonlocal coupling, given by Eq. (2). The elements λ of the spectrum of the resulting linear operator represent the growth rates of small perturbation around the original wave. A possible instability is reflected by the presence of eigenvalues with positive real parts. In what follows we shortly describe the method of computing the spectrum of a given travelling wave.

As shown in the Appendix , we can cast the Oregonator equations with nonlocal coupling in the form of the following reaction-diffusion equation

$$T\partial_t u = F(u) + D\partial_{xx}u, \quad u\in\mathbb{R}^3, \tag{3}$$

where D is a diagonal diffusion matrix with non-negative elements and $F(u)$ incorporates the nonlinear Oregonator kinetics and the nonlocal coupling terms. The matrix T accounts for the fact that the equation for the nonlocal field (A3) has no time dependence, i.e., we set $T=\mathrm{diag}(1,1,0)$.

In the frame $z=x-ct$ which moves with the velocity c we obtain from Eq. (3),

$$T\partial_t u = F(u) + cT\partial_z u + D\partial_{zz}u. \tag{4}$$

The profile $u(z)$ of travelling waves with constant velocity and shape is thus governed by the following ODE:

$$Du'' + cTu' + F(u) = 0, \tag{5}$$

where the prime denotes a derivative with respect to the comoving coordinate $z=x-ct$.

We consider first the stability of periodic pulse trains $u_L(z)=u_L(z+L)$. The eigenvalue problem is then given by the following system:

$$\lambda Tw = \partial_u F[u_L(z)]w + cTw' + Dw'', \quad w\in\mathbb{C}^3,$$

$$(w,w')(L) = e^{i2\pi\gamma}(w,w')(0). \tag{6}$$

We say that λ is in the spectrum of the wave train $u_L(z)$, if Eq. (6) has a bounded solution for some $\gamma\in\mathbb{R}$ [23,29,30]. In order to obtain the spectrum of a given wave train, we solve the boundary-value problem (6) using the continuation software AUTO [31,32]. The spectrum comes up in curves $\lambda=\lambda(i\gamma)$ in the complex plane. Note that $\lambda=0$ with the eigenfunction given by $w(z)=u_L'(z)$ (the so-called Goldstone mode) is always in the spectrum due to the translation symmetry of the problem.

For $L\to\infty$ the spectrum of periodic wave trains exponentially converges to the spectrum of solitary pulses [29]. For wave trains of large spatial period, there is a circle of critical eigenvalues attached to origin, which can be thought of as a blow-up of the isolated Goldstone eigenvalue of the solitary pulse [33]. Given the solitary pulse is stable, the location of this circle of critical eigenvalues (either in the left or right complex half-plane) describes the stability and interaction of pulses in wave trains with large wavelengths.

We calculated the leading parts of spectrum of wave trains belonging to the different parts of the dispersion curve with an overshoot, see Fig. 2. The wave trains on the part of dispersion with positive slope $dc/dL>0$ are found to be stable [Fig. 2(b)]. As predicted by the theory [23], at the extremum of the dispersion curve $dc/dL=0$ we obtain spectrum with

$$\frac{d}{d(i\gamma)}\,\mathrm{Im}(\lambda)\bigg|_{\lambda=0} = 0,$$

compare Fig. 2(c). Moving along the dispersion curve further, we observe a long-wavelength instability of wave trains, which is characterized by

$$\frac{d^2}{d(i\gamma)^2}\,\mathrm{Re}(\lambda)\bigg|_{\lambda=0} = 0,$$

see Fig. 2(d). In Fig. 2(e) we present the spectrum of periodic wave train which undergoes the period-doubling bifurcation. We read from the spectrum that $\lambda=0$ is twofold degenerated, for the second eigenfunction we find $\gamma=0.5$, which means that this eigenfunction has period $2L$. Exactly at this point, the branch of wave trains of doubled wavelength emerges from the primary dispersion curve.

Both L-periodic and $2L$-periodic wave trains are found to be unstable on unbounded domains for wavelengths larger

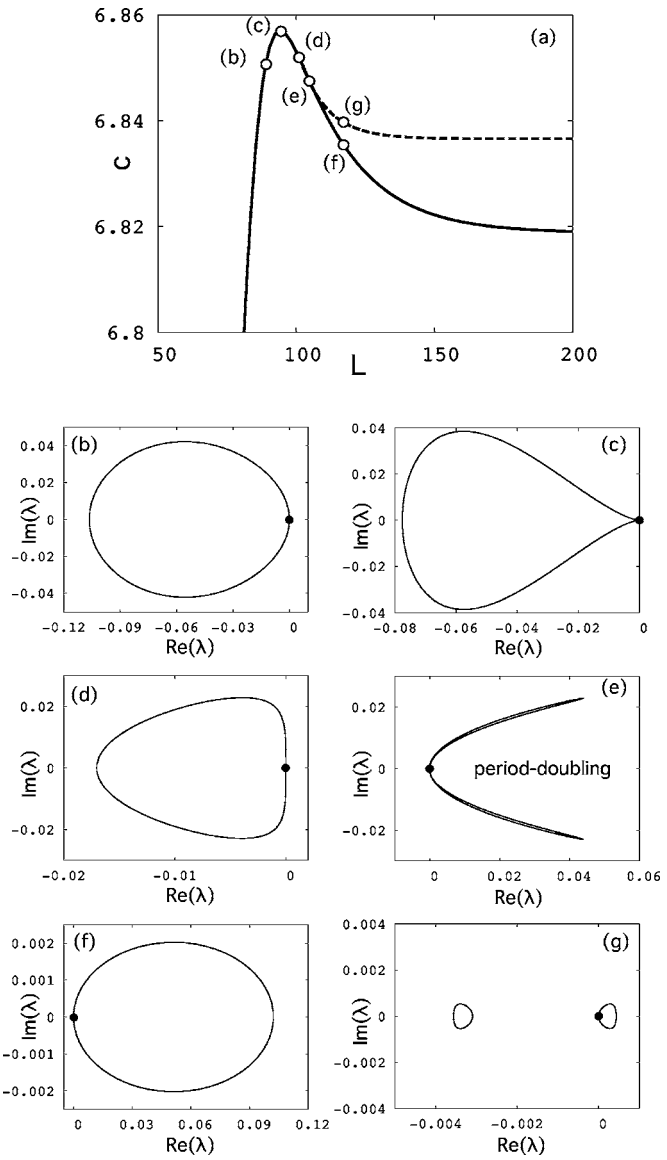

FIG. 2. Stability of bound states for $\mu=-8.0\times10^{-3}$. (a) Dispersion curve of periodic pulse trains, displaying an overshoot. Velocity of L-periodic ($2L$-periodic) wave trains is shown by the solid (dashed) line, respectively. Empty dots (b)–(g) denote the points for which the essential spectrum was computed. (b)–(g) The corresponding essential spectra.

than the wavelength of the period-doubling bifurcation, see Figs. 2(f) and 2(g), where the circle of critical eigenvalues belongs to the right half-plane. The instability of periodic wave trains reflects the attractive interaction between the pulses within a train, which causes a breakup of periodic structure and formation of pulse pairs. However, as $L\to\infty$ the critical circle of eigenvalues shrinks to the Goldstone eigenvalue $\lambda=0$, and solitary pulses and bound states are thus stable.

For $2L$-periodic wave trains we found another part of the spectrum in the left half-plane [Fig. 2(g)], which shrinks to a point eigenvalue for $L\to\infty$, i.e., for a solitary bound state. This point eigenvalue of the bound state can be thought of as the eigenvalue of the *weak interaction* between two pulses in the bound state [22]. In general, however, the interaction eigenvalue can belong to the right half-plane, making the bound state unstable. We refer to Sec. III F for a more general discussion of the stability of bound states.

III. GENERAL DESCRIPTION OF CASE $\mu=0$

The aim of this section is to show that the emergence of bound states that are induced by nonlocal coupling is model independent. We show that a solitary pulse undergoes a certain bifurcation at $\mu=0$ and that this bifurcation produces bound states regardless of the specific underlying kinetics of the reaction-diffusion system.

A. Profile equations with nonlocal coupling

We consider a reaction-diffusion system in one spatial dimension with N species and kinetics f,

$$\partial_t u = f(u,\phi(x)) + D\partial_{xx}u, \quad u\in\mathbb{R}^N \tag{7}$$

with a diffusion matrix $D=\mathrm{diag}(d_j), j=1,\ldots,N$. The field $\phi(x)$ represents nonlocal coupling given by

$$\phi(x) = \phi_0 + \mu\int_{-\infty}^{\infty} e^{-\sigma|y|}[u_i(x+y)-u_i(x)]dy, \tag{8}$$

where we take the ith species of u to construct $\phi(x)$. Again, the value σ^{-1} is considered to be large.

We refer to the Appendix for the construction of the diffusion equation for the field $\phi(x)$. Solutions to Eq. (7) in the form of $u(z)=u(x-ct)$ in the comoving coordinate z are thus governed by the following profile equations:

$$u'' + cu' + f(u,\phi(u_i,X;\mu)) = 0,$$

$$X'' - \sigma^2 X + u_i = 0,$$

where the prime denotes a derivative with respect to z. X and ϕ are related through

$$\phi(u_i,X;\mu) = \phi_0 + 2\mu\left[\sigma X(x) - \frac{u_i(x)}{\sigma}\right].$$

We cast the profile equation as a first-order system,

$$U' = F(U,\Phi(U,Z;\mu);c), \quad U\in\mathbb{R}^{2N},$$

$$Z' = AZ - BU, \quad Z\in\mathbb{R}^2, \tag{9}$$

where

$$A = \begin{pmatrix} 0 & 1 \\ \sigma^2 & 0 \end{pmatrix}.$$

Functions $\Phi(U,Z;\mu)$ and $F(U,\Phi(U,X;\mu);c)$ are obtained from given $\phi(u,X;\mu)$ and $f(u,\phi(u,X;\mu))$ in a straightforward way. The matrix B accounts for the coupling between the appropriate components of U and Z. Nonlocal coupling effectively extends the phase space of the profile equation in a linear way by two dimensions. The asymptotic flow in the Z subspace is given by the simple equation

$$Z'_{\pm} = \pm \sigma Z_{\pm}, \tag{10}$$

where $Z_{\pm}$ are the eigenvectors of the matrix A.

In our following analysis we consider the case $\mu=0$. We assumed that without nonlocal coupling the reaction-diffusion system supports propagation of stable solitary pulses. This means that there exist a homoclinic solution $(U^0,Z^0)(z)$ to the profile equation

$$U' = F(U,\phi_0;c),$$

$$Z' = AZ - BU, \tag{11}$$

with some $c=c_0$. Then the linearization of Eq. (11) around $(U^0,Z^0)(z)$,

$$v' = \mathcal{A}(z)v, \quad v \in \mathbb{C}^{2N+2}, \tag{12}$$

has a bounded solution given by $v(z)=\partial_z(U^0,Z^0)(z)$. The adjoint linearized problem

$$\psi' = -\mathcal{A}^*(z)\psi, \quad \psi \in \mathbb{C}^{2N+2} \tag{13}$$

has a bounded solution as well [23]. The solution of the adjoint variational equation is perpendicular to the tangent spaces of the stable and unstable manifolds of the equilibrium, which is used in order to define the orientation of the homoclinic orbit later on.

The Jacobian matrix of Eq. (9) in the fixed point for $\mu=0$ is given by

$$\mathcal{A}(0) = \begin{pmatrix} \partial_U F(0,\phi_0;c) & 0 \\ -B & A \end{pmatrix}. \tag{14}$$

The eigenvalues of $\mathcal{A}(0)$ are exactly those of the matrices $\partial_U F(0,\phi_0;c)$ and A. The leading eigenvalues of $\mathcal{A}(0)$ (those with smallest real parts) are then $\pm\sigma$ (see inset in Fig. 4) and the corresponding leading eigenvectors are given by

$$(\underbrace{0,\ldots,0}_{2N},1,\pm\sigma)^T.$$

Note that in the case $\mu=0$ the leading eigenvectors are always perpendicular to the U subspace, this corresponds to the fact that the profile of $u(x)$ is not affected by the variable $\phi(x)$ for $\mu=0$.

B. Codimension-2 bifurcations of homoclinic orbits

Now let us recall three general assumptions on the homoclinics of codimension one to a saddle equilibrium with real eigenvalues $-\lambda_{ss}<-\lambda_s<0<\lambda_u$ [24]:

(1) the leading eigenvalues are not in resonance $\lambda_u \neq \lambda_s$,

(2) the solution $v(z)$ to the linearized problem Eq. (12) converges to zero along the leading eigenvectors of the linearization in the fixed point, and

(3) the same applies to the solution $\psi(z)$ of the adjoint problem Eq. (13).

The last assumption is sometimes called *the strong inclination property*, for homoclinics in $\mathbb{R}^3$ it means that the two-dimensional stable manifold comes in backward time tangent to the strong stable direction of the fixed point (see Fig. 3). A

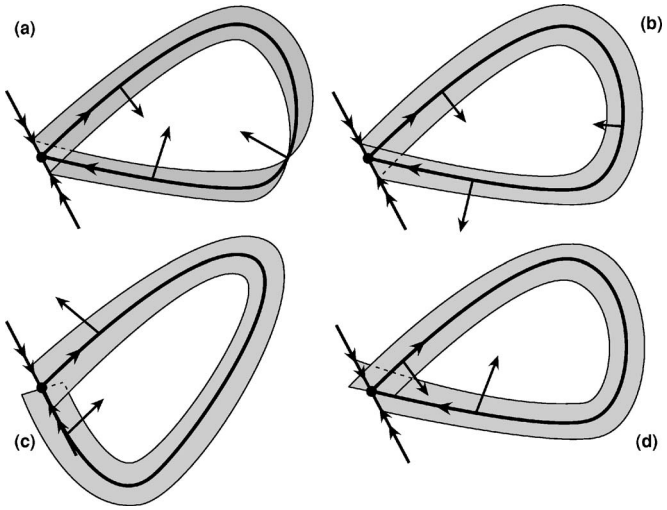

FIG. 3. Sketches of homoclinic orbits. Filled circles denote the equilibrium. Leading directions are shown by single arrows, strong stable direction is shown by doubled arrows. Arrows perpendicular to the homoclinics indicate the solution to the adjoint variational equation. The gray strip shows the stable manifold of the fixed point close to the homoclinic orbit. (a) Generic codimension-1 orientable homoclinic orbit. (b) Generic codimension-1 twisted homoclinic orbit. (c) Codimension-2 orbit flip of homoclinic orbit. (d) Codimension-2 inclination flip of homoclinic orbit.

homoclinic orbit of codimension-1 can be orientable or twisted, depending on the orientation of the strip of the two-dimensional manifold, see Figs. 3(a) and 3(b). One defines the *orientation* $\mathcal{O}$ of a given homoclinic orbit with the help of the solution $\psi(z)$ to the adjoint variational equation (13) as

$$\mathcal{O} = \lim_{z\to\infty} \operatorname{sgn}\langle\psi(z),v(-z)\rangle \cdot \langle\psi(-z),v(z)\rangle, \tag{15}$$

where $v(z)$ denotes the solution to the linearized equation (12).

If one of the above assumptions is violated, one speaks of codimension-2 bifurcations of homoclinic orbits [24]. These are, in the order of the assumptions above,

(1) resonance homoclinic orbit,

(2) orbit flip, and

(3) inclination flip.

The resonance bifurcation can produce 2-homoclinics and both flip bifurcations can produce 2- and N-homoclinics. A branch of period-doubling bifurcation emerges from the bifurcation point as well [see Figs. 3(c), 3(d), and 4 for a qualitative picture of a codimension-2 bifurcation and the emergence of 2-homoclinics]. In orbit (inclination) flip bifurcation, the vector $v(z)$ $[\psi(z)]$ for $z\to\pm\infty$ switches through the strongly stable eigenspace of $\mathcal{A}(0)$, respectively. Both flip bifurcations correspond to the change of the sign of the scalar products that contribute to the orientation $\mathcal{O}$ and can be detected as zeroes of the orientation.

In our analysis of the effect of nonlocal coupling on the pulse dynamics we are particularly interested in the inclination flip. Let us recall the details of the inclination flip bifurcation of a homoclinic orbit in $\mathbb{R}^3$ to a saddle with one-dimensional unstable and two-dimensional stable manifold

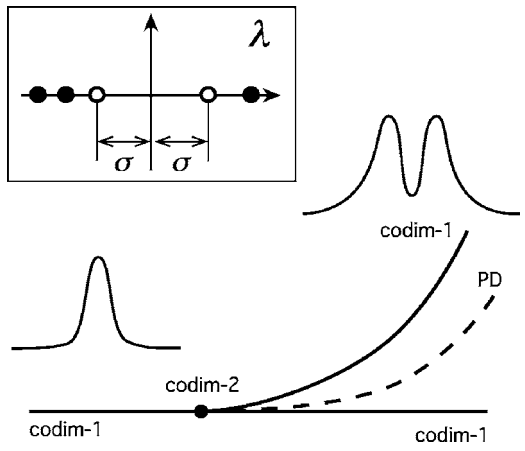

FIG. 4. A codimension-2 bifurcation of a homoclinic orbit, the emergence of a 2-homoclinic orbit (solid line) and a period-doubling bifurcation *PD* (dashed line). Inset: Empty circles denote the eigenvalues of the matrix A, full circles show the eigenvalues of $\partial_U F(0,\phi_0;c)$.

[see Fig. 5(a)]. Before and after the bifurcation the solution of the adjoint variation equation approaches zero along the leading eigenvector, as mentioned above. The two-dimensional stable manifold approaches the saddle point in backward time tangent to the strongly stable eigenvector. In the bifurcation point the solution of the adjoint equation picks the nonleading eigenvector of the linearization in the equilibrium for $z\to-\infty$. The two-dimensional stable manifold approaches the equilibrium in the backward time tangent to the weakly stable eigenvector.

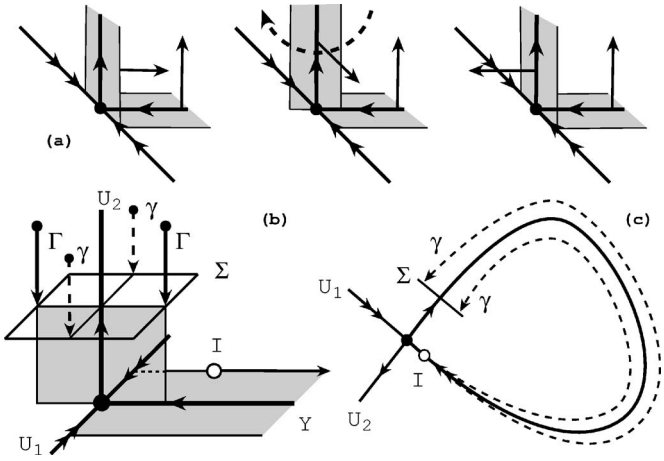

FIG. 5. (a) Details of inclination flip bifurcation. Left panel: stable 2D manifold of the fixed point before the bifurcation. Middle panel: stable 2D manifold in the bifurcation point, note that the solution to the adjoint equation is directed along the strongly stable direction. Right panel: the same 2D stable manifold after the bifurcation. (b) Illustration of the inclination flip in the extended system (18). Empty dot I shows the initial condition in the stable manifold for the integrating in backward time, Σ shows the Poincaré section, γ denotes the unfeasible hypothetic trajectories that start in the phase point I, and Γ denotes the feasible trajectories, see the text. (c) Projection of the homoclinic orbit in Eq. (18) on the U subspace. I, Σ, and γ have the same meaning as in (b).

C. Resonance and inclination flips for $\mu=0$

We can immediately see that nonlocal coupling for $\mu=0$ breaks the first assumption, since the leading eigenvalues $\pm\sigma$ of the linearization (14) are obviously in resonance.

The second assumption about the asymptotics of the homoclinic orbit holds. It physically means that the nonlocal field decays in space much slower than the u-profile of the pulse.

The strong inclination property is violated at $\mu=0$ with respect to both stable and unstable manifolds. It means that the homoclinic orbit that describes a solitary pulse in the absence of nonlocal coupling undergoes two inclination flip bifurcations if considered in the phase space extended by the coupling variable Z in Eq. (11). Let us consider the adjoint variational equation (13) together with Eq. (14) for $\mu=0$

$$\begin{pmatrix} U \\ Z \end{pmatrix}' = -\begin{pmatrix} \partial_U F^*(U(z),\phi_0;c) & -B^* \\ 0 & A^* \end{pmatrix}\begin{pmatrix} U \\ Z \end{pmatrix}. \tag{16}$$

We see that the Z subsystem is completely decoupled from the U part. The equation for Z' is simply given by

$$Z' = -A^* Z, \quad A^* = \begin{pmatrix} 0 & \sigma^2 \\ 1 & 0 \end{pmatrix}, \tag{17}$$

and the variable U has no influence on the flow of Z, which is the counterpart of the fact that in the linearized equation (12) the U subsystem is not affected by Z.

We seek for a solution $(U,Z)(z)$ to Eq. (16), which vanishes for large z, i.e., $(U,Z)\to 0$ as $z\to\pm\infty$. For a codimension-1 homoclinic orbit, we expect that this solution approaches zero along the leading eigenvectors of $-\mathcal{A}^*(0)$, given by $(0,\ldots,0,1,\pm\sigma)^T$. However, the only bounded solution to Eq. (17) for $z\to\pm\infty$ is given by $Z=0$, which means that the solution $(U,Z)(z)$ to Eq. (16) must pick the nonleading eigenvectors of $\mathcal{A}(0)$, given by $(U^\pm,0,0)^T$, in order to converge to zero for $z\to\pm\infty$. Here, $U^\pm$ represents the leading eigenvectors of the matrix $\partial_U F^*(U(z),\phi_0;c)$.

Finally we write

$$\psi(z) = \begin{pmatrix} U^\pm \\ 0 \\ 0 \end{pmatrix} e^{\mp\sigma z}, \quad \text{for } z\to\pm\infty$$

for the solution $\psi(z)$ of the adjoint problem and

$$v(z) = \begin{pmatrix} 0 \\ 1 \\ \pm\sigma \end{pmatrix} e^{\mp\sigma z}, \quad \text{for } z\to\pm\infty$$

for the solution $v(z)$ of the linearized problem, given by Eq. (12). Substituting the above expressions for $v(z)$ and $\psi(z)$ in Eq. (15)

$$\mathcal{O} = \lim_{z\to\infty} \operatorname{sgn}\langle\psi(z),v(-z)\rangle\cdot\langle\psi(-z),v(z)\rangle,$$

we immediately see that both scalar products vanish, rendering two inclination flips with respect to the stable and the unstable manifolds.

D. Geometrical interpretation

We simplify the problem, exploring the extension of the profile equation only by one stable direction Y,

$$U' = F(U, \phi_0; c),$$

$$Y' = -\sigma Y - BU. \tag{18}$$

We are interested in the behavior of the stable manifold of the equilibrium of Eq. (18) in backward time.

We emphasize once again that we work with nonlocal coupling switched off, i.e., $\mu=0$, and assume that there exists a homoclinic orbit in the U subsystem of Eq. (18). This implies that in the extended system there exists a homoclinic orbit as well, and the homoclinic orbit in the extended system approaches the equilibrium along the Y direction, since the Y axis is the leading stable eigenvector to the leading eigenvalue $-\sigma$ of the Jacobian of Eq. (18).

We refer to Fig. 5(b) for the geometry of the eigendirections and the stable manifold in the system. Our idea is to compare the full phase space of the extended system with its projection on the U variables, where the actual dynamics takes place. The U subspace of Eq. (18) is decomposed in the leading unstable direction U_2 and the strongly stable eigendirection U_1. The leading stable eigendirection is Y.

We choose a Poincaré section Σ across the leading unstable eigenvector close to the equilibrium. Next, we set an initial condition [marked by I in Fig. 5(b)] close to the homoclinic orbit in the two-dimensional stable manifold, and follow it in backward time along the homoclinic orbit. An important question is how this trajectory returns to the previously chosen Poincaré section. For a generic codimension-1 homoclinic orbit, the trajectory from our initial condition returns along one of the dashed lines with the arrows marked by γ in Fig. 5(b). In the projection on the U plane it would mean, however, that the trajectory does not remain on the homoclinic orbit, which is impossible because the starting point belongs to the homoclinic orbit in the U subspace, which in turn is an invariant trajectory [see Fig. 5(c) for the projections of the hypothetical trajectory marked by γ]. In other words, the U components of our hypothetical trajectory must be the original homoclinic orbit in the original profile equation

$$U' = F(U, \phi_0; c)$$

without nonlocal coupling. Last means that the feasible trajectory of point I in backward time must come to the section Σ along the vectors marked by Γ.

Comparing Fig. 5(a) and 5(b), we conclude that for $\mu=0$ our system displays an inclination flip with respect to the stable manifold. In exactly the same way one can show an inclination flip with respect to the unstable direction while considering the extension of the profile equation by one unstable direction (with $+\sigma$),

$$U' = F(U, \phi_0; c),$$

$$Y' = \sigma Y - BU. \tag{19}$$

In this case the same considerations can be applied, keeping in mind that Y becomes now the leading unstable direction of Eq. (19) and Fig. 5(b) can be used with the reversed directions of the arrows.

E. Summary: Codimension-4 homoclinic orbit

Summarizing our results for $\mu=0$, we find a codimension-4 homoclinic orbit in the profile equation for travelling waves in the reaction-diffusion system (7) with nonlocal coupling given by Eq. (8). Here, we present the list of the bifurcations together with the assumptions, under which we find the degeneracies.

(1) Inclination flip with respect to the stable manifold [extended Eq. (18)]. Assumption: $-\sigma$ is the leading stable eigenvalue of $\mathcal{A}(0)$, i.e., the matrix $\partial_U F(0, \phi_0; c_0)$ has no eigenvalues with the real part between $-\sigma$ and 0.

(2) Inclination flip with respect to the unstable manifold [extended Eq. (19)]. Assumption: σ is the leading unstable eigenvalue of $\mathcal{A}(0)$, i.e., the matrix $\partial_U F(0, \phi_0; c_0)$ has no eigenvalues with the real part between 0 and σ.

(3) Resonance condition for the leading eigenvalues $\pm\sigma$. Assumption: the matrix A has a specific form, given by Eq. (10). This can be violated, for example, by the choice of temporarily inertial nonlocal coupling like in Ref. [34].

(4) Existence of the homoclinic orbit itself (existence of solitary pulse in PDE for $\mu=0$). Assumption: there exists a solitary pulse without nonlocal coupling.

We would like to stress that the high codimension of the bifurcation at $\mu=0$ does not depend on the particular system and is solely provided by the nonlocal coupling. The first two assumptions can be fulfilled by the choice of sufficiently large coupling range, i.e., by the smallness of σ, while the third one follows naturally from the symmetry of the coupling function $e^{-\sigma|y|}$. In this sense the high codimension of the solitary pulse at $\mu=0$ and the bifurcation to pulse pairs is a generic feature of systems with nonlocal coupling.

Three of the four bifurcation are unfolded upon switching on nonlocal coupling by setting $\mu \neq 0$. Each of the found homoclinic bifurcations can produce 2-homoclinic orbits, see Tables I and II in Ref. [25]. Bifurcations to 2-homoclinic orbit for the profile equation (11) corresponds to the emergence of bound states with two pulses with the same velocity in the full PDE system. All three bifurcations were precisely detected numerically in the Oregonator model at $\mu=0$ by the continuation software AUTO [32].

F. Stability of bound states

Stability of the bifurcating bound states can be determined in the general framework of the stability of multibump pulses [22]. Under assumption of large interpulse distance the interaction of the pulses within a bound state is weak and can be estimated from the decay properties of the corresponding solitary pulse.

Suppose that we have found a bound state for $\mu=\mu_0$ close to $\mu=0$. The interpulse distance L_p in the bound state is considered to be large. To simplify our analysis, we assume

that the leading eigenvalues of the matrix $\mathcal{A}(0)$ for $\mu=\mu_0$ are given by $\nu^s<0$ and $\nu^u>0$, where $\nu^u>-\nu^s$. The last means that the exponential wake behind the pulse decays slower that in the front of it, which is quite often the case if the velocity of the pulse is not zero. The critical spectrum of the bound state with two pulses is then given by two point eigenvalues, one of which is necessarily $\lambda=0$, representing the translation invariance of the pulse pair.

The second eigenvalue describes the interaction of pulses within a bound state and thus decides upon the stability of the pulse pair. Under the above assumptions on the matrix $\mathcal{A}(0)$, this eigenvalue is given by [22,23]

$$\lambda_i = -\frac{1}{M}\langle \psi(L_p/2), v(-L_p/2)\rangle,$$

where M is the Melnikov integral for the solitary pulse, $v(z)$ and $\psi(z)$ are the solutions to the linear equations (12) and (13) for the solitary pulse.

The easiest way to determine the sign of λ_i is to check the stability of periodic pulse trains with interpulse distance L_p. The sign of

$$-\frac{1}{M}\langle \psi(L_p/2), v(-L_p/2)\rangle$$

decides upon the stability of periodic pulse trains as well [33]. Equivalently, the location of the circle of the critical eigenvalues is determined by the above scalar product.

As a result, a pulse pair with interpulse distance L_p is stable if the corresponding spatially periodic pulse train with the same wavelength is stable. For large wavelengths, there is a relation between the slope of the dispersion $c(L)$ and the stability of wave trains, which says that for $\frac{d}{dL}c(L)>0$ the wave trains are stable [8]. Thus it is possible to predict the stability of the bound state from the slope of the dispersion curve for the appropriate periodic pulse trains with the wavelength $L=L_p$.

IV. DISCUSSION AND OUTLOOK

In this paper, we have shown that nonlocal coupling in the form of exponentially decaying connections between the elements of the medium leads to the emergence of bound states of pulses. The results of our analysis were obtained under general assumptions on the underlying equations and thus are applicable to a wide class of reaction-diffusion systems under influence of nonlocal coupling with exponentially decaying strength.

The central point of our analysis was the case where the coupling strength μ was equal to zero. The homoclinic orbit which describes the solitary pulse for $\mu=0$ was shown to be of codimension-4. Upon switching on nonlocal coupling, the homoclinic orbit became a generic one of codimension-1. This unfolding of the codimension-4 bifurcation leads to the emergence of N-homoclinics that correspond to bound states in the reaction-diffusion system with nonlocal coupling. Our results also apply to a nonlocal coupling with a sufficiently small temporal inertiality τ [34]; in this case the matrix A in Eq. (9) is slightly different and the leading eigenvalues of A are not in resonance anymore. We would still have a codimension-3 homoclinic orbit, which can bifurcate to double pulses.

We stress that the high codimension of the bifurcation is provided essentially by the form of the nonlocal coupling and does not depend on the particular properties of the pulses in the reaction-diffusion system. In our numerical computation with continuation software the predicted bifurcations were accurately detected, which can be considered as a numerical proof of the theoretical analysis. Additionally, in the numerically investigated example the bound state has been shown to be linearly stable, which can be seen as a first step towards real experimental verification of the results.

There are still some open questions about the considered bifurcations. We have shown two inclination flips and resonant homoclinic orbit simultaneously for $\mu=0$. Both flip bifurcation and resonance condition can produce 2-homoclinics and so far it is not clear which specific bifurcation leads to the emergence of bound states. The interplay of two inclination flip bifurcations with the resonance condition assures an even more intriguing dynamical behavior than near a codimension-3 point [26,27].

ACKNOWLEDGMENTS

The authors thank Dmitry Turaev and Georg Röder for discussions and criticisms. This work was supported by DFG in the framework of SFB 555.

APPENDIX: DIFFUSION EQUATION FOR THE COUPLING FIELD

Here, we derive the equation for the coupling field $\phi(x)$, which is given by

$$\phi(x) = \phi_0 + \mu\int_{-\infty}^{\infty} e^{-\sigma|y|}[u_i(x+y) - u_i(x)]dy, \qquad \text{(A1)}$$

where $u_i(x)$ is the ith species of the original reaction-diffusion equation. We rewrite the coupling field in the form

$$\phi(x) = \phi_0 + \mu\int_{-\infty}^{\infty} e^{-\sigma|y|}u_i(x+y)dy - \mu\int_{-\infty}^{\infty} e^{-\sigma|y|}u_i(x)dy$$

$$= \phi_0 + 2\mu\left(\sigma X(x) - \frac{u_i(x)}{\sigma}\right). \qquad \text{(A2)}$$

Using the Fourier transform

$$\int_{-\infty}^{\infty} e^{-\sigma|y|}e^{-iky}dy = \frac{2\sigma}{\sigma^2+k^2},$$

it is not hard to see that the function $X(x)$ obeys the following linear differential equation:

$$X_{xx} = \sigma^2 X - u_i. \qquad \text{(A3)}$$

[1] M. Cross and P. C. Hohenberg, Rev. Mod. Phys. **65**, 851 (1993).
[2] A. S. Mikhailov, *Foundation of Synergetics I: Distributed Active Systems* (Springer, Berlin, 1991).
[3] J. Christoph, M. Eiswirth, N. Hartmann, R. Imbihl, I. Kevrekidis, and M. Bär, Phys. Rev. Lett. **82**, 1586 (1999).
[4] N. Manz, S. C. Müller, and O. Steinbock, J. Phys. Chem. A **104**, 5895 (2000).
[5] V. K. Vanag and I. R. Epstein, Phys. Rev. Lett. **88**, 088303 (2002).
[6] N. Manz, C. T. Hamik, and O. Steinbock, Phys. Rev. Lett. **92**, 248301 (2004).
[7] N. Manz and O. Steinbock, Phys. Rev. E **70**, 066213 (2004).
[8] M. Or-Guil, I. G. Kevrekidis, and M. Bär, Physica D **135**, 154 (2000).
[9] M. Abeles, *Corticonics* (Cambridge University Press, England, 1991).
[10] G. Ermentrout and J. Cowan, Biol. Cybern. **34**, 137 (1979).
[11] J. Christoph and M. Eiswirth, Chaos **12**, 215 (2002).
[12] F. Plenge, H. Varela, and K. Krischer, Phys. Rev. Lett. **94**, 198301 (2005).
[13] M. Barahona and L. M. Pecora, Phys. Rev. Lett. **89**, 054101 (2002).
[14] D. M. Abrams and S. H. Strogatz, Phys. Rev. Lett. **93**, 174102 (2004).
[15] S. I. Shima and Y. Kuramoto, Phys. Rev. E **69**, 036213 (2004).
[16] Y. Kuramoto, D. Battogtokh, and H. Nakao, Phys. Rev. Lett. **81**, 3543 (1998).
[17] E. Nicola, Ph.D. thesis, Technische Universität Dresden, 2001.
[18] E. M. Nicola, M. Or-Guil, W. Wolf, and M. Bär, Phys. Rev. E **65**, 055101(R) (2002).
[19] M. Hildebrand, H. Skødt, and K. Showalter, Phys. Rev. Lett. **87**, 088303 (2001).
[20] E. M. Nicola, M. Bär, and H. Engel, Phys. Rev. E **73**, 066225 (2006).
[21] *Chemical Waves and Patterns*, edited by R. Kapral and K. Showalter (Kluwer Academic, New York, 1995).
[22] B. Sandstede, Trans. Am. Math. Soc. **350**, 429 (1998).
[23] B. Sandstede, *Stability of Travelling Waves* (North-Holland, Amsterdam, 2002).
[24] Y. A. Kuznetsov, *Elements of Applied Bifucation Theory* (Springer, Berlin, 1995).
[25] B. Sandstede, J. Dyn. Differ. Equ. **9**, 269 (1997).
[26] B. E. Oldeman, B. Krauskopf, and A. R. Champneys, Nonlinearity **14**, 597 (2001).
[27] A. Homburg and B. Krauskopf, J. Dyn. Differ. Equ. **12**, 749 (2000).
[28] H.-J. Krug, L. Pohlmann, and L. Kuhnert, J. Phys. Chem. **94**, 4862 (1990).
[29] B. Sandstede and A. Scheel, Physica D **145**, 233 (2000).
[30] B. Sandstede and A. Scheel, Phys. Rev. E **62**, 7708 (2000).
[31] J. Rademacher, B. Sandstede, and A. Scheel, URL http://www.wias-berlin.de/people/rademach/specnum-subm.pdf
[32] E. Doedel, R. Paffenroth, A. Champneys, T. Fairgrieve, Y. Kuznetsov, B. Oldeman, B. Sandstede, and X. Wang, AUTO2000: Continuation and bifurcation software for ordinary differential equations (with HOMCONT), Concordia University, Montreal, 2002.
[33] B. Sandstede and A. Scheel, J. Differ. Equations **172**, 134 (2001).
[34] D. Tanaka and Y. Kuramoto, Phys. Rev. E **68**, 026219 (2003).